

Received January 11, 2022, accepted February 6, 2022, date of publication February 8, 2022, date of current version March 4, 2022.

Digital Object Identifier 10.1109/ACCESS.2022.3150017

# Economic and Stable Operation of Meshed MTDC/AC Grid as Affected by the Spatiotemporal Complementarities of Geographically Dispersed Wind Generation

JING ZHOU<sup>1</sup>, YI LIU<sup>1</sup><sup>2</sup>, ZHE KANG<sup>1</sup>, AND ZHUOYU JIANG<sup>1</sup>

<sup>1</sup>Three Gorges Power Company Ltd., Yichang 443000, China

<sup>2</sup>Beijing Lingyang Weiye Technology Company Ltd., Beijing 100176, China

Corresponding author: Yi Liu (1159170349@qq.com)


This work was supported by the Research Project of China Three Gorges Corporation under Grant 202103521.

**ABSTRACT** Complementarities of geographically dispersed wind resources have been well recognized and evaluated based on the statistics of wind data. This paper investigates the effect of spatiotemporal complementarities of grid-connected offshore wind farms on operational cost and stability of meshed DC/AC grids with VSC-based MTDC networks. The investigation is carried out for a real power system in Jiangsu Province, China, and has used the real hourly wind data provided by the China Meteorological Administration (CMA) in terms of the unit commitment (UC) as well as the probabilistic small-signal angular stability. Several distributed offshore wind farms are interconnected via a VSC-based MTDC network to send power to the southern area in Jiangsu Province. Computational results of the UC and system probabilistic stability demonstrate that significant saving of operational cost and stability improvement can be brought about from the complementarities of geographically distributed offshore wind farms.

**INDEX TERMS** Wind power, complementarities, small-signal stability, unit commitment, MTDC, smoothing effect, monte carlo simulation.

## I. INTRODUCTION

Wind power poses significant challenges to the economic and stable operation of power system. First, wind energy tends to be geographically dispersed and far from load centers. Second, electric output from wind generations is highly variable due to the intermittent and fluctuant nature of wind. Hence, integrating of wind power into power systems may cause a series of new problems for power system economic and stable operation. The focus of work presented in this paper is to demonstrate the positive impact of utilizing spatiotemporal complementarities [1] of dispersed wind resources on power system operation and stability. It is shown in the paper that wind complementarities effectively smooth the stochastic variations of wind power, which reduces the operational cost of power system and enhances system stability.

The associate editor coordinating the review of this manuscript and approving it for publication was Youngjin Kim .

The fact that geographically dispersed wind generation is complementary has been well known for a while. For example, as early as in 1979, Kahn [2] used statistical approaches to evaluate the reliability of wind generators and concluded that the reliability increases as a function of geographic dispersal of wind turbines. After that, a growing body of literature has carried out the examinations of complementarities of dispersed wind resources. For example, authors of the Occident studies [3]–[6] found improvement in the steadiness of the available power and a decrease in the number of low- or no-wind events [7], even when the interconnection of wind resources over regions is as small as a few tens of kilometers apart. Interconnecting wind generations for longer separation distances yields less variability, which means fewer times of the very low power and the highest power [8]. For instance, a recent study [9] simulates wind power from 11 wind sites, distributed over a 2,500 km extent along the U.S. east coast, and found that power output from the entire set of generators rarely reaches either low or full power, and power changes

slowly when compared with each individual site. Based on hourly wind speed data, authors of [10] and [11] found that the variability of hour-to-hour energy production decreases significantly when interconnecting dispersed wind farms in China.

However, so far wind complementarities have been carried out by use of the methods of mathematical statistics as briefly reviewed above. No published work has explicitly examined the complementarities of geographically dispersed wind generation under the operational environment of a real power system. Part of the reasons are that up to now, wind generation has been developed mainly in small scale and close to low or middle voltage (LV or MV) networks for local consumption. In this case, effect of spatiotemporal complementarities of wind generation is not very obvious and crucial to the economic operation and stability of the power system.

Effects on the power system economic and stable operation brought about by wind power have been a rich area for research. Main cost component of wind integration occurs in the unit commitment (UC) time frame [12]. In [13]–[15], a UC program was adopted to determine wind power's impact on a thermal system operation. Those studies have made a significant contribution to the formulation of the UC of power systems involving wind power and provided valuable insight into the influence of wind power on power system economic operation. However, the focus of study on the UC has been about handling wind power dispatch effectively. Rarely the impact of different wind profiles on the UC has been noted explicitly. In addition, to the best knowledge of authors, no special study has examined in detail the impact of complementarities of dispersed wind resources on the economic operation of power systems in terms of the UC. As far as the power system stability as affected by the variability of wind generation is concerned, several previous studies [16]–[18] indicate that with the increase of penetration level of grid-connected wind generation, risk brought about by the random fluctuation of wind power output to power system stable operation increases significantly. However, none of those studies have investigated in detail the stability of power systems as affected by the complementarities of geographically dispersed wind generation.

The focus of this paper is the investigation of wind complementarities under the operational environment of a real power system in China. The effect of wind complementarities are examined in two aspects: (1) on cost saving of power system operation with grid-connected wind in terms of the UC; (2) on power system probabilistic stability improvement as the result of smoothing function of complementarities to the stochastic drifting of operating point of the power system caused by random variation of grid-connected wind power. Available methods of the UC and probabilistic stability assessment are adopted to obtain and compare the estimation of operational cost and system probabilistic stability of complementary and non-complementary cases. The results confirm the benefits of wind complementarities found previously from wind data manipulation by calculation

of operational cost and stability analysis of the real power system.

In China, wind energy locates mainly in the remote western and north-western areas as well as eastern coast. It is an enormous challenge to transfer large-scale wind generation from those areas though relatively weak national ac networks to the load centers in the east and south of China. Hence it is anticipated that majority of remote large-scale wind farms in China will be connected to main ac network through HVDC lines [19]. This will provide opportunity to develop a multi-terminal DC (MTDC) network for long-distance transmission of large-scale wind power in China, which itself has been a very much hot topic of discussion recently for the large-scale offshore wind power transmission in the North Sea. The MTDC network for large-scale wind power transmission provides the way to maximize the spatiotemporal complementarities of geographically dispersed wind generation.

Jiangsu Province in China has a long coastline where wind energy resources are abundant. According to [20], the potential installed capacity is high at a height of 50 meters above sea level in the shallow seas with a 5- to 25-meter water depth along coast. Such plentiful wind power will be transmitted with HVDC lines to the load centers into the Jiangsu power grid (JPG). In this paper, the spatiotemporal complementarities of geographically dispersed wind generation are evaluated for JPG. The paper is organized as follows. Section II builds the evaluation model of economic and stable operation of meshed MTDC/AC system with the complementarities of dispersed wind generation being considered. Section III presents the real JP (Jiangsu Province) power system and models the wind power based on real wind data collected. Section IV gives the results of evaluation of effect of wind complementarities on the economic operation and stability of JPG respectively in terms of wind power UC and probabilistic small-signal stability considering wind fluctuations. Conclusions are Section V at the end of the paper.

## II. EVALUATION MODEL OF WIND COMPLEMENTARITIES

### A. OPERATIONAL COST OF MESHED MTDC/AC SYSTEM IN TERMS OF UC AS AFFECTED BY THE WIND COMPLEMENTARITIES

#### 1) MODELING FORECAST UNCERTAINTIES

The dominant cost component of wind integration occurs in the UC, which is to generate a most economic day-ahead schedule of conventional power generation to meet load and wind variations. A bibliographical survey of UC problem is presented in [21]. The UC problem comes from two sources: generation units' outages and forecasting errors. As the purpose of study in this paper is to obtain an estimation of operational cost of wind integration in terms of the UC so as to compare cases of complementary and non-complementary wind generation, the work is focused on the latter, namely forecast errors of wind power and load demand as it is in [19]. The dispatch interval and the horizon of day-ahead scheduling are 1 h and 24 h, respectively. The effort is to examine

the cost saving brought about by wind complementarities via comparison of operational cost between complementary and non-complementary cases rather than to enhance the precision of the UC, available methods proposed in the literature are used to formulate the UC procedure adopted by this paper.

Hourly day-ahead forecast of load ( $L_{d,f,t}$ ) and wind power ( $W_{d,f,t}$ ) are modeled as equation (1) and (2), respectively where  $P_{L,t}^{Mean}$  and  $P_{W,t}^{Mean}$  are expected load demand and wind power, respectively.  $e_{L,t}$  and  $e_{W,t}$  are the forecast errors of load and wind power, respectively.

$$L_{d,f,t} = P_{L,t}^{Mean} + e_{L,t} \quad (1)$$

$$W_{d,f,t} = P_{W,t}^{Mean} + e_{W,t} \quad (2)$$

where  $P_{L,t}^{Mean}$  and  $P_{W,t}^{Mean}$  are expected load demand and wind power, respectively.  $e_{L,t}$  and  $e_{W,t}$  are the forecast errors of load and wind power, respectively.

$e_{L,t}$  and  $e_{W,t}$  [22] are all modeled as a zero-mean normally distributed random variation. The standard deviation of  $e_{L,t}$  ( $\sigma_{L,t}$ ) is considered as a percentage (2% in this work) of the expected power load demand, a simplification as the previous UC study [23]. The standard deviation of  $e_{W,t}$  ( $\sigma_{W,t}$ ) normally increases with the prediction horizon increases, decreases with the growing of the number of turbines within a farm and the region diameter [24]. However, within the same region the decreasing of  $\sigma_{W,t}$  due to the increase in the number of wind turbines quickly reaches a saturation level controlled by the region diameter [25]. For an ensemble of wind farms in a region with a diameter of 140 km, the standard deviation of wind power forecast error ( $\sigma_{W,140km}^t$ ) with a 24 hour horizon can be plotted as a function of the normalized predicted wind power as equation (3)

$$\sigma_{W,140km}^t = \frac{1}{50}I_W + \frac{1}{5}P_{W,t}^{Mean} \quad (3)$$

where  $I_W$  is the installed wind power capacity.

When the region diameter ( $d$ , km) (it was observed that the dependency from the number of sites within each region was not significant) changes, the standard deviation of  $e_{W,t}$  ( $\sigma_{W,t}^d$ ) is expressed by equation (4)

$$\sigma_{W,t}^d = \mu\sigma_{W,140km}^t \quad (4)$$

where  $\mu$  varies with the change of  $d$ , referring to [24], [26]. Wind power in UC is modeled as negative load demand

$$L_{d,f,t}^{net} = L_{d,f,t} - W_{d,f,t} = L_{net,t}^{Mean} + e_{net,t} \quad (5)$$

In which,  $L_{d,f,t}^{net}$  is the day-ahead forecast net load,  $L_{net,t}^{Mean}$  is the expected net load,  $e_{net,t}$  is the forecast error of net load.

As there is no correlation between wind power and load forecast errors [27], the standard deviation ( $\sigma_{net,t}$ ) is got by (6)

$$\sigma_{net,t} = \sqrt{(\sigma_{W,t}^d)^2 + (\sigma_{L,t})^2} \quad (6)$$

Based on the probabilistic rule described in [28], power reserve requirements ( $R_{res,t}$ ) used to deal with forecasting

uncertainties in this paper can be given as

$$R_{res,t} = \varepsilon\sigma_{net,t} \quad (7)$$

Here  $\varepsilon = 3$ , which means 99.74% of variations are covered [28].

## 2) MATHEMATICAL FORMULATION OF UC PROBLEM

The objective of UC is to minimize the operation cost of power system as expressed in equations (8)-(10). Equation (9) is the generation cost function, which is accurately modeled by a set of piecewise blocks as introduced in [29]. As in [30], a two-segment startup cost function is applied as shown in (10).

$$Obj = \text{Min} \sum_{t=1}^T \sum_{i=1}^{N_g} [CC_{i,t}(P_{i,t}^g) + CS_{i,t}^g] \quad (8)$$

$$CC_{i,t}(P_{i,t}^g) = a_i + b_i \times (P_{i,t}^g) + c_i \times (P_{i,t}^g)^2 \quad (9)$$

$$CS_{i,t}^g = \begin{cases} s_{i,t}HSC_i & \text{if } U_{i,t}^{off} < CST_i \\ s_{i,t}CSC_i & \text{if } U_{i,t}^{off} \geq CST_i \end{cases} \quad (10)$$

where

$N_g$	Number of generation units
$T$	Number of hours in the scheduling period
$CC_{i,t}$	Generation cost function of unit $i$
$CS_{i,t}^g$	Startup cost function of unit $i$
$P_{i,t}^g$	Power output from unit $i$
$a_i, b_i, c_i$	Coefficients of the cost function of unit $i$
$s_{i,t}$	A binary variable for start-up status of unit $i$
$HSC_i$	Hot start-up cost
$CSC_i$	Cold start-up cost
$U_{i,t}^{off}$	Number of hours the unit was turned off
$CST_i$	Threshold value of hours for hot and cold start

The objective function is subject to the following constraints:

### $a$ : GENERATION CONSTRAINTS

Equation (11) is the minimum and maximum power output constraints. Equation (12) presents the ramp rate limits of generation. The minimum up time constraints of unit  $i$  are presented by equations (13)-(15). The minimum down time constraints of a unit are expressed by equations (16)-(18).  $G_i$  in equation (13) and  $L_i$  in equation (16) can be mathematically expressed as equation (19) and (20), respectively.

$$u_{i,t}P_{g,i}^{Min} \leq P_{i,t}^g \leq u_{i,t}P_{g,i}^{Max} \quad (11)$$

$$-60 \times RR_i^g \leq P_{i,t}^g - P_{i,t-1}^g \leq 60 \times RR_i^g \quad (12)$$

$$\sum_{t=1}^{G_i} (1 - u_{i,t}) = 0 \quad (13)$$

$$\sum_{s=t}^{t+T_i^{on}-1} u_{i,s} \geq T_i^{on}(u_{i,t} - u_{i,t-1}) \quad \forall t = G_i + 1, \dots, T - T_i^{on} + 1 \quad (14)$$

$$\sum_{s=t}^T [u_{i,s} - (u_{i,t} - u_{i,t-1})] \geq 0 \quad \forall t = T - T_i^{on} + 2, \dots, T \quad (15)$$

$$\sum_{t=1}^{L_i} (1 - u_{i,t}) = 0 \quad (16)$$

$$\sum_{s=t}^{t+T_i^{off}-1} (1 - u_{i,s}) \geq T_i^{off}(u_{i,t-1} - u_{i,t}) \quad \forall t = L_i + 1, \dots, T - T_i^{off} + 1 \quad (17)$$

$$\sum_{s=t}^T [1 - u_{i,s} - (u_{i,t-1} - u_{i,t})] \geq 0 \quad \forall t = T - T_i^{off} + 2, \dots, T \quad (18)$$

$$G_i = \text{Min} [T, (T_i^{on} - T_{i,0}^{on})u_{i,0}] \quad (19)$$

$$L_i = \text{Min} [T, (T_i^{off} - T_{i,0}^{off})(1 - u_{i,0})] \quad (20)$$

where

- $P_{g,i}^{\text{Min}}$  Lower boundary of power output of unit  $i$
- $P_{g,i}^{\text{Max}}$  Upper boundary of power output of unit  $i$
- $RR_i^g$  Power ramp rate of unit  $i$
- $u_{i,t}$  A binary variable for the committed status of unit  $i$
- $G_i$  Initial periods during which unit  $i$  must be online
- $T_i^{on}$  Minimum online time of unit  $i$
- $T_{i,0}^{on}$  The periods during which unit  $i$  has been online prior to the first period of the time span
- $u_{i,0}$  Initial commitment state of unit  $i$ .
- $L_i$  Initial periods during which unit  $i$  must be offline
- $T_i^{off}$  Minimum offline time of unit  $i$
- $T_{i,0}^{off}$  Periods during which unit  $i$  has been offline prior to the first period of the time span

### b: SECURITY CONSTRAINTS OF MESHED MTDC/AC NETWORKS

Fig.1 depicts a general configuration of a hybrid AC/MTDC networks. Security constraints should be imposed on the whole MTDC/AC grid. On AC grid side, ignoring the line losses a DC power flow model [31] as expressed in Equation (21) is applied to ensure the supply-demand balance. Equation (22) ensures that the AC lines are not over loaded. On MTDC grid side, Equation (23) without considering the DC line losses ensures the power flow balance of MTDC network. Equation (24) presents the constraints of converter DC voltage level. Equation (25) ensures that the

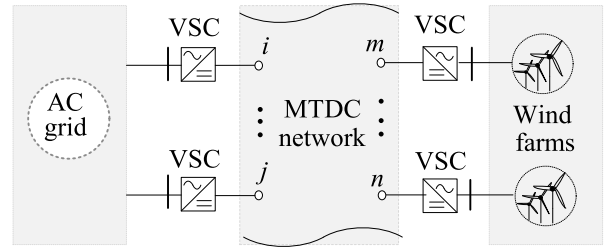


FIGURE 1. Configuration of hybrid AC/VSC-MTDC system.

DC lines are not over loaded. A V-I control method [19] is used by the MTDC converters and the DC power can be calculated using equations (26). In the case of a VI - droop, the power injected into DC bus can be written as equation (27). Equation (28) presents the power limitations of the DC converters. Equation (29) gives the spinning reserve constraint.

$$P_{e,t}^g - L_{e,t} + P_{sm,t} = \sum_f \frac{1}{X_{ef}} (\theta_{f,t} - \theta_{e,t}) \quad (21)$$

$$-P_{ef}^{\text{Max}} \leq \frac{1}{X_{ef}} (\theta_e - \theta_f) \leq P_{ef}^{\text{Max}} \quad (22)$$

$$P_{dcm,t} = \sum_n \frac{1}{R_{mn}} (U_{dcm,t} - U_{dcm,t}) \quad (23)$$

$$U_{dc}^{\text{min}} \leq U_{dc,t} \leq U_{dc}^{\text{max}} \quad (24)$$

$$-P_{mn}^{\text{Max}} \leq \frac{1}{R_{mn}} (U_{dcm,t} - U_{dcm,t}) \leq P_{mn}^{\text{Max}} \quad (25)$$

$$P_{dcm,t} = \begin{cases} -P_{sm,t} & \text{V-I droop bus} \\ P_{m,t}^w & \text{Wind power injection bus} \end{cases} \quad (26)$$

$$P_{dcm,t} = k_m (U_{dcm,t} - U_{dcm,0}) \quad (27)$$

$$-P_{con}^{\text{Max}} \leq P_{dcm,t} \leq P_{con}^{\text{Max}} \quad (28)$$

$$\sum_{i=1}^{N_g} (u_{i,t} \times P_{g,i}^{\text{Max}}) + L_{net,t}^{\text{Mean}} \geq R_{res,t} \quad (29)$$

where

- $P_{e,t}^g$  Total power generated by all the units at AC bus  $e$
- $L_{e,t}$  Load demand at AC bus  $e$

$P_{sm,t}$	Power injected into bus AC bus $e$ from MTDC grid
$\theta_{e,t}$	Power angle at AC bus $e$
$\theta_{f,t}$	Power angle at AC bus $f$
$X_{ef}$	Reactance of the AC line connecting bus $e$ and $f$
$P_{ef}^{Max}$	Capacity of the AC line connecting bus $e$ and $f$
$P_{m,t}^w$	Accommodated wind power at DC bus $m$
$R_{mn}$	Resistance of DC line connecting bus $m$ and $n$
$U_{dc}^{max}$	Maximal limit of DC voltage
$U_{dc}^{min}$	Minimal limit of DC voltage
$U_{dc,t}$	Voltage of DC bus
$P_{dcm,t}$	Power injected into DC bus
$P_{mn}^{Max}$	Capacity of the DC line connecting bus $m$ and $n$
$k_m$	V-I droop, defined as $\Delta I_{dc}/\Delta U_{dc}$
$U_{dcm,0}$	Initial voltage of DC bus
$P_{con}^{Max}$	Power limitation of DC converter

*c: WIND POWER CONSTRAINT*

Wind power curtailment may occur due to the network constraints, hence in this paper wind power curtailment is considered. In this case, the power injected into DC bus can be written as equation II-B

$$0 \leq P_{dcm,t} \leq P_{dcm,t}^{Mean} \quad (30)$$

where  $P_{dcm,t}^{Mean}$  is the expected wind power at the DC bus.

3) UC SOLUTION

The UC problem is model as a linear mixed integer problem in a GAMS environment [32] and the CPLEX solver is applied to solve it. Fig.2 shows the computational flowchart of the simulation method which uses the rolling planning

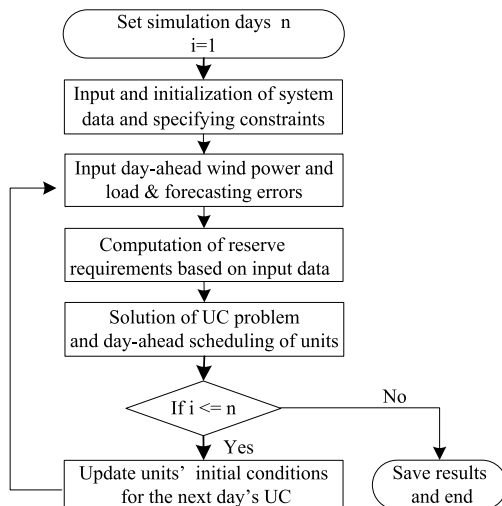


FIGURE 2. Flowchart of the simulation method.

technique [33] to quantify the influence of the complementary effect of dispersed wind resources.

**B. PROBABILISTIC SMALL SIGNAL ANGULAR STABILITY OF MESHED MTDC/AC SYSTEM AS AFFECTED BY THE WIND COMPLEMENTARITIES**

Power system small-signal angular stability is affected by the stochastic fluctuations of grid-connected wind generation. For a power system being considered stable deterministically, there may still exist certain probability that the system can lose stability as the result of random variations of wind power output [34]. The risk brought about by the stochastic fluctuations of grid-connected wind can be assessed by the probabilistic stability of power systems. Random variations of wind penetration lead to the stochastic drifting of power system operating points which changes mode positions of power systems. The sensitivity of the eigenvalue against wind power can be used to assess how the wind power affects the mode position.

Wind complementarities smooth the fluctuations of wind generation which may result in less stochastic drifting of power system operating points. Thus utilization of wind complementarities may improve the probabilistic small-signal stability of a power system as compared to the case of non-complementarities. This benefit of wind complementarities to the stable operation of power systems is evaluated in this paper. The focus of study here is the evaluation of effect of wind complementarities on power system stability by comparing complementary and non-complementary wind generation rather than accurate assessment or enhancement of system stability. Hence a simple one-order excitation system has been employed for all the synchronous generators. Examination of PSS design and assignment onto HVDC stations are not considered. However, in the study, full dynamic model of generators, DFIG and rotor-side converter controller are used (parameters are given in Appendix A).

A procedure of applying Monte Carlo simulation to assess the effect of grid-connected wind generation on AC power system probabilistic small-signal rotor angle stability is proposed in [35]. The probability density function (PDF) of the real part of critical oscillation mode of a power system is calculated firstly. Then probabilistic small-signal angular stability of the power system can be computed. The Monte Carlo simulation procedures of probabilistic small signal stability analysis for meshed MTDC/AC system adopted by this paper are given in Fig.3.

**III. TEST REAL POWER SYSTEM AND MODELING WIND POWER BASED ON REAL WIND DATA**

**A. REAL TEST POWER SYSTEM**

The test power system used in this paper is the power transmission system in Jiangsu Province (JSP), China. The HV (500 kV) JSP power grids are illustrated in Fig.4. The system has 160 synchronous generators and 45 buses. The generation capacity of the system is 66.6k MW and the annual peak

TABLE 1. Generation data.

Number of units	Unit code	Fuel type	$P_{g,i}^{Min}$ (MW)	$P_{g,i}^{Max}$ (MW)	$RR_i^g$ (MW/min)	$T_i^{on}$ (h)	$T_i^{off}$ (h)	$CST_i$ (h)	$HSC_i$ ( $10^4$ ¥)	$CSC_i$ ( $10^4$ ¥)	$a_i$ (¥/h)	$b_i$ (¥/MWh)	$c_i$ (¥/MW <sup>2</sup> h)
10	U120	Gas	60	120	3	5	4	5	7	14	7040	10.65	1.35
6	U137	Coal	68.5	137	2	5	4	4	6..5	13	3192.1	85.9	1.00
6	U250	Hydro	50	250	100	-	-	-	-	-	0.006	0.006	0
16	U300	Coal	150	300	6	5	4	8	10	20	1062.5	126.25	0.20
26	U330	Coal	165	330	6	5	4	8	10	20	7447.8	57.1	0.35
34	U350	Coal	175	350	6	5	4	8	10	20	504.15	132.55	0.15
7	U398	Gas	199	398	7	6	4	9	12	24	1490.1	114.8	0.20
50	U600	Coal	300	600	10	6	4	10	13	26	15300	21.55	0.20
3	U100	Coal	500	1000	20	9	4	12	15	30	25833	16.45	0.10
2	N100	Nuclear	500	1000	50	-	-	-	-	-	2372.7	26.52	0.0013

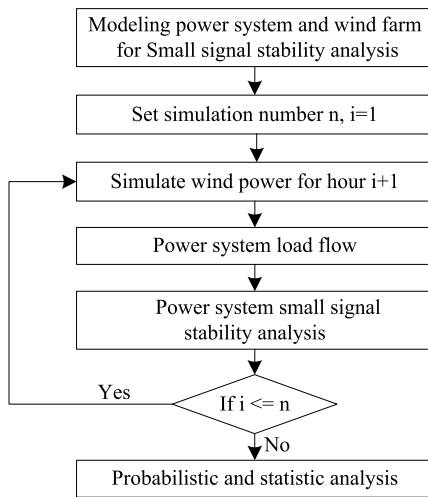


FIGURE 3. Flowchart of Monte Carlo for probabilistic small signal stability analysis.

load is 64.7kMW. Details of generation of some key generators for the UC simulation are presented in Table 1. Wind resources along the eastern coastline of Jiangsu Province are redundant which has been identified as one of the main sites to develop large-scale offshore wind generation in China. Shandong Province is the neighbor province in the north of Jiangsu where rich offshore wind resources are available. This paper studies how system economic operation of JPG (Jiangsu Province Grid) is affected by the wind complementarities of dispersed wind generation in terms of the UC, when large-scale offshore wind farms are fully developed at southeastern (WF1) and northeastern (WF2) area along the coastline of Jiangsu Province as well as at the sea along the coastline of Shandong Province (WF3) as shown in Fig.4.

In order to investigate the benefits brought about by wind complementarities, wind power transmission over the sea water through voltage source converter (VSC) based HVDC technology is considered and combined wind power output is achieved through a multi-terminal DC (MTDC) network as shown in Fig.4. Load center in Jiangsu Province locates at

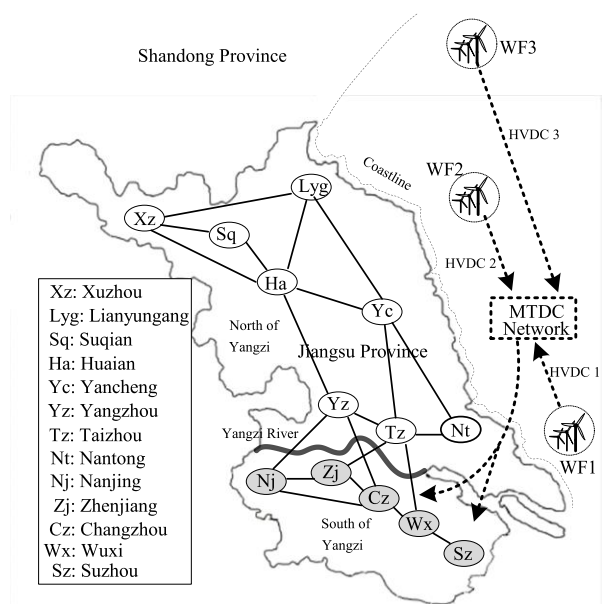


FIGURE 4. Configuration of JPG.

the southern area of Yangzi River. Hence in the study, offshore wind power is considered to be sent to the 500kV buses of the highlighted areas in the south of Yangzi River as shown in Fig.4. The meshed MTDC/AC network is depicted in Fig.5.

The models of meshed MTDC/AC system and wind power generator for small signal stability analysis are given in Appendix A.

### B. MODELING WIND POWER BASED ON REAL WIND DATA

As in [10], [11], this paper uses the real wind speed at the height of 10m provided by China Meteorological Administration (CMA) to simulate electric power from the wind farm at a given site. The available hourly wind data are from Oct.1 2009 to Sept.31 2010. Offshore wind speed at the measurement height are adjusted to the hub-height by using the logarithmic law [36] as given in equation (31) with

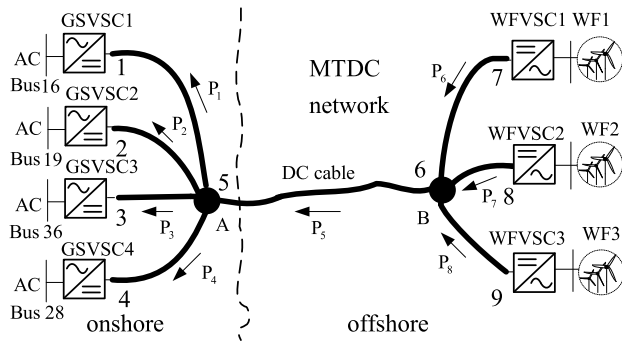


FIGURE 5. Network of meshed MTDC/AC system.

a roughness length  $L_0 = 0.0002$  m, which varies little for different sea areas and is recommended as an average value for calm and open seas [37].

Some observed wind data from onshore sites near the sea are transformed into the inferred offshore data by using the following equation IV

$$V_{hub} = V_{sea} \left( \frac{\ln(H_{hub}) - \ln(L_0)}{\ln(H_0) - \ln(L_0)} \right) \quad (31)$$

$$V_{sea} = 1.62 + 1.17V_{land} \quad (32)$$

where  $V_{hub}$  is the wind speed at the hub height  $H_{hub}$ ,  $H_0$  is the measurement reference height, 10 m in this paper,  $V_{land}$  is the measured onshore wind speed.

The power-curve can be used to simulate electric power output  $P$  of a single wind turbine. This curve maps the hub-height wind speed to turbine power, i.e.  $P = f(V_{hub})$ , which is supplied by the manufacturer. Varied power curve for different wind turbines and wind farms may have smoothing effect on power output. However, the sensitivity of studies on the hourly complementary impact of wind recourses to wind turbine type is only a few percent [9], [38]. Hence only one wind turbine type, A Chinese mainstream 3MW wind turbine type, Sinovel SL 3000/90, is assumed to be installed in every wind farm. The normal parameters for this wind turbine type are given in Appendix B.

Atmospheric turbulence may have a certain effect on the power output from wind farms. The WAsP model [39] used for the velocity deficit in offshore wind farm is given as follows

$$U_{wake} = U_{free} \left[ 1 - \left( 1 - \sqrt{1 - C_T} \right) \left( \frac{D}{D + 2k_{wake}X_d} \right)^2 \right] \quad (33)$$

where  $C_T$  is the thrust coefficient,  $X$  is the downstream distance from the turbine,  $D$  is the rotor diameter of the turbine,  $U_{free}$  is the free-stream wind speed, and  $k_{wake}$  is a wake decay constant, of which the suggested value is 0.05 for offshore wind farm [40].

## IV. TEST RESULTS

### A. UC OF MESHED MTDC/AC SYSTEM AS AFFECTED BY THE WIND COMPLEMENTARITIES

In order to demonstrate and compare, the following possible scenarios of offshore wind power supply are considered in the test Jiangsu power system

- (1) WF1: only the offshore wind farm in the southern sea along the coastline of Jiangsu Province supplies power to the load in the south of Yangzi River.
- (2) WF2: only the offshore wind farm in the northern sea along the coastline of Jiangsu Province supplies power to the load in the south of Yangzi River.
- (3) WF1+WF2: two wind farms along the coastline of Jiangsu Province send power to the load in the south of Yangzi River through the MTDC network.
- (4) WF1+WF2+WF3: three wind farms along the coastline of Jiangsu and Shandong Province send power to the load in the south of Yangzi River through the MTDC network.

For the UC simulation total wind power ( $P_5$ ) received by the hub A (see fig.5) are transmitted to the four AC buses in proportion to their amount load demands (in this work,  $n_1 : n_2 : n_3 : n_4 = 3 : 2 : 5 : 3$ ) by adjusting  $k_m$  of DC converters, of which the derivation is shown in Appendix C. Note that within scenario (3) and (4), installed wind capacity at each site is same.

At first, one week wind power profiles and the highest weekly load power for JPG are considered. The selected weekly capacity factor of all profiles is taken as 0.264, which means that the average production of each wind farm is 26.4% of their installed capacity. Table 2 shows the simulation results when the wind penetration level is 30%. Two cases are considered: 1) without MTDC transmission limits, MTDC system has the ability to transmit all the produced wind power. In such case wind power curtailment just occur due to the limits of AC system; 2) with MTDC transmission limits, the capacity of MTDC line connecting hub A and B (see Fig.5) is set to be 65% of wind installed capacity. In this case both the constraints of AC and DC system may effect wind power curtailment.

Results in Table 2 shows that different wind profiles have different impact on the UC, even when wind facilities are in a relative small region. Interconnecting dispersed wind farms could reduce operational cost and wind power curtailments. During low load periods, wind power curtailment may occur to ensure that sufficient generation units are online to guarantee adequate  $R_{res,t}$  to accommodate net load fluctuation. In such case, the higher wind power is, the more curtailed wind power is. Interconnecting dispersed wind farms could reduce the possibility of very-high wind output events, which is concluded by previous research. In addition, single wind farm hourly power fluctuates faster. In such case it needs higher ramping capabilities of AC system, which will also influence the on-or-off states of generation units, especially in low load periods. When interconnecting dispersed wind farms, power fluctuates slowly and less  $R_{res,t}$  is needed to

**TABLE 2. Weekly operational cost when the wind penetration is 30%.**

Scenario	Without MTDC transmission limits			
	WF1	WF2	WF1+WF2	WF1+WF2+WF3
Operational cost (10 <sup>9</sup> RMB)	1.2589	1.2579	1.2498	1.2405
Curtailed wind (10 <sup>4</sup> MWh)	5.0333	4.1165	2.6549	2.0784
Scenario	With MTDC transmission limits			
	WF1	WF2	WF1+WF2	WF1+WF2+WF3
Operational cost (10 <sup>9</sup> RMB)	1.2664	1.2596	1.2525	1.2419
Curtailed wind (10 <sup>4</sup> MWh)	10.543	5.4765	5.2849	2.7184

accommodate net load due to higher forecast precision. Furthermore, there are fewer hours when power generation is at high level when interconnecting dispersed wind farms.

Fig.6 shows wind curtailment when not taking the constraints of DC system into consideration. From Fig.6, it can be see that when the transmission capacity of MTDC is set to 65% of total generated wind power, more wind power curtailment may occur, when compared with no-MTDC-limit scenario. In other words, lower DC line capacity means more wind curtailment. However, when considering wind complementary effect, a certain wind power discard may bring significant investment saving of DC lines. Hence in practice, it is wise to allow a certain wind power curtailment to save the cost to raise transmission capacity of long-distance DC lines and power transmission efficiency, especially when interconnecting dispersed wind farms to supply power to load center. To study the optimization of MTDC network structure by considering transmission line capacity and sites of wind farms to maximize the economic benefits brought about by the complementary effect of dispersed wind farms, it needs to carry out simulation over a long period of time. Our paper just provides a new way to investigate the economic effect of meshed MTDC/AC transmission systems to include the effect of wind complementarities.

For each scenario, the UC for every month was carried out by using the rolling algorithm illustrated in the above section and yearly operational cost was computed. Table 3 gives the results of operational cost in different scenarios of offshore wind connections when the level of wind penetration is 30%. From Table 3 it can be seen that making use of complementarities of offshore wind generation at different locations (WF1+WF2+WF3) can bring about yearly operation saving  $1.226 \times 10^9$  RMB (as compared with WF1+WF2),  $1.45 \times 10^9$  RMB (as compared with WF1) and  $1.526 \times 10^9$  RMB (as compared with WF2) respectively. If the level of wind penetration reaches 30%, total yearly operational saving from making use of wind complementarities (WF1+WF2+WF3) will be  $2.504 \times 10^9$  RMB or  $2.88 \times 10^9$  as compared to WF1 or WF2 only. Note that wind farms within each scenario share

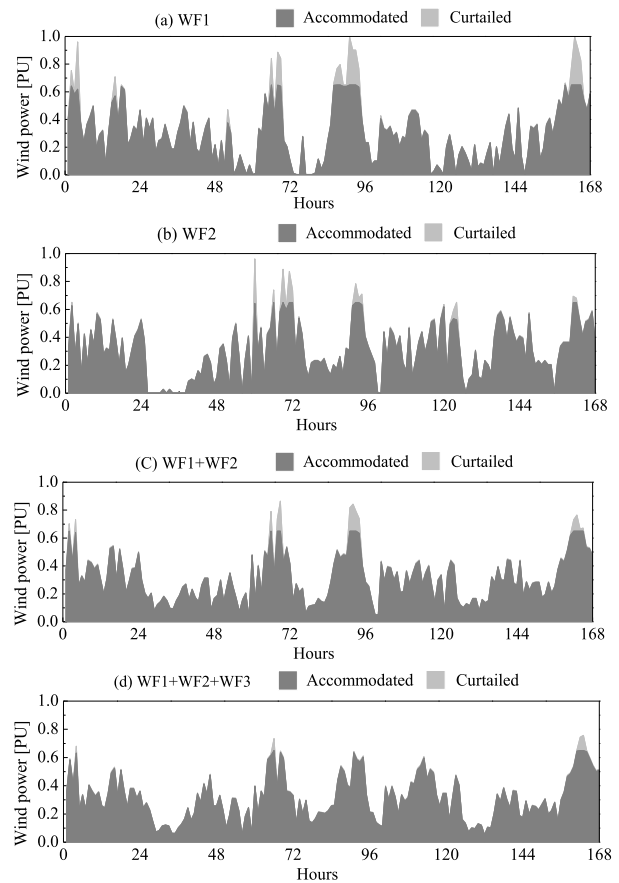


**FIGURE 6. Curtailed against accommodated wind power when MTDC constraints are considered with wind power penetration level at 30%.**

**TABLE 3. Yearly operational cost when the wind penetration is 20%.**

Scenario	Without MTDC transmission limits			
	WF1	WF2	WF1+WF2	WF1+WF2+WF3
Operational cost (10 <sup>10</sup> RMB)	6.3944	6.402	6.372	6.2494

wind capacity equally. Note that the capacity factors of these wind farms are 0.342, 0.338 and 0.351, respectively.

Fig.7 shows the yearly operational cost of the system plotted against different levels of wind power penetration. It can be seen from Fig.7 that

- (1) When the offshore wind farm in one area supplies wind power to Jiangsu Province (WF1 or WF2 alone), the operational cost decreases more slowly with the increase of penetration level of wind power. The trend of decrease approaches even saturation when the penetration level is over 35%.
- (2) Complementarities of two offshore wind farms bring down the yearly operational cost (WF1+WF2). The higher the penetration level of wind power, the more the yearly operational cost is saved.



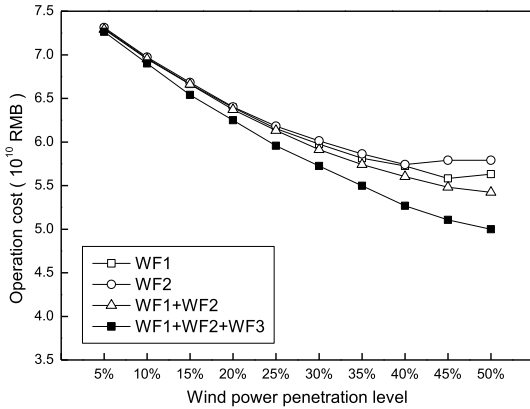


FIGURE 7. Operational cost versus wind power penetration level.

- (3) The best scenario is when the offshore wind in Shandong is brought in (WF1+WF2+WF3). Significant yearly operational cost can be saved from the complementarities of offshore wind farms. The decrease speed of operational cost does not reduce evidently even when the penetration level of wind power reaches 50%.

**B. PROBABILISTIC SMALL SIGNAL ANGULAR STABILITY OF MESHED MTDC/AC SYSTEM AS AFFECTED BY THE WIND COMPLEMENTARITIES**

It is well-known that the spatiotemporal complementarities of geographically distributed wind generation have the effect of smoothing the random variations of wind power output. Hence it is highly possible that the complementarities may reduce the risk from the stochastic fluctuations of grid-connected wind generation on power system small-signal angular stability. This aspect of benefit of complementarities of wind generation has been examined in the test power system of Jiangsu Province and is presented as follows.

The Monte Carlo simulation has been used to calculate the PDF of the critical oscillation mode of the test power system. Results given below were obtained when the level of wind penetration is 20%.

**1) TEST SYSTEM OPERATES UNDER A NORMAL LOADING CONDITION**

Under a normal loading condition, it was identified that the critical oscillation mode of the test power system is  $\lambda_{critical} = -0.1981 \pm j3.9422$  from the deterministic small-signal stability analysis. Hence deterministically, the system is stable and the mode is well damped with a damping ratio of 5.02%.

For different possible scenarios of offshore wind farm connections, the PDFs of the damping ratio of the critical oscillation mode of the test power system were calculated by use of Monte Carlo simulation and displayed in Fig.8. From Fig.8 it can be seen that although power output from WF1 or WF2 exhibits dramatically power ups and downs, wind complementarities (WF1+WF2+WF3) has made the real part of the critical oscillation mode more locate in the middle, more

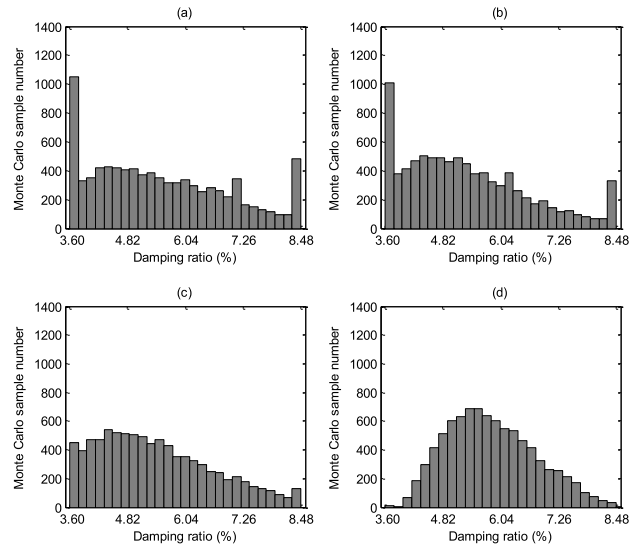


FIGURE 8. PDF of damping ratio of system critical oscillation mode for different scenarios of offshore wind power supply (A): (a) WF1 only; (b) WF2 only; (c) WF1+WF2; (d) WF1+WF2+WF3.

analogue to the PDF of a normal distribution. This means that the spatiotemporal complementarities of geographically dispersed wind sites can reduce the probability of very low or high power events sharply, which is the anticipated feature of smoothing effect of the spatiotemporal complementarities.

From the PDFs displayed in Fig.8, probability that the critical oscillation mode of the test power system is well damped (damping ratio  $\geq 5.0\%$ ) was computed and is given in Table 4. From the results in Table 4 is can be seen that the spatiotemporal complementarities of combined wind power supply (WF1+WF2+WF3) indeed give the best chance that the critical oscillation mode is well damped.

TABLE 4. Probability of damping ratio of critical oscillation mode  $\geq 10\%$ .

Wind power supply scenario	WF1	WF2	WF1+WF2	WF1+WF2+WF3
Probability of damping ratio $\geq 5.0\%$	58.93%	54.48%	58.14%	84.97%

The distribution of the PDFs of damping ratio of system is quite similar to that of wind turbine mechanical power. There exist two distinct concentrations of probability masses in the distribution for WF1 and WF2: the left one corresponds to the situation that the wind farm is cut off; the right one corresponds to situation that wind turbine generates rated power. However, when connecting geographically dispersed wind generations, the PDFs of damping ratio have changed: both the left and right distributions decrease. This is because the number of zero- or full-wind events decreases due to the complementarities of dispersed wind generation, thus the aggregate power rarely reaches the rated power or zero power. For WF1+WF2+WF3, probability masses concentrates in

the middle range, and the PDFs for it are similar to a normal distribution.

2) TEST POWER SYSTEM OPERATES AT A STRESSED LOADING CONDITION

At a stressed loading condition, the critical oscillation mode of the test power system is  $\lambda_{critical} = -0.0122 \pm j3.9168$ . Deterministically, the system is stable, though very close to the static stability limit. Fig.9 shows the computational results of PDFs of the damping ratio of the critical oscillation mode. From the PDFs, probabilistic small-signal stability of the test power system was computed and results are presented in Table 5.

From the results in Table 5 it can be seen that though the system is considered stable deterministically, there exists the risk that the system becomes unstable. This risk is reduced by the spatiotemporal complementarities of combined wind power supply (WF1+WF2+WF3), as the probability of system being stable increases when power output from different offshore wind farms is combined.

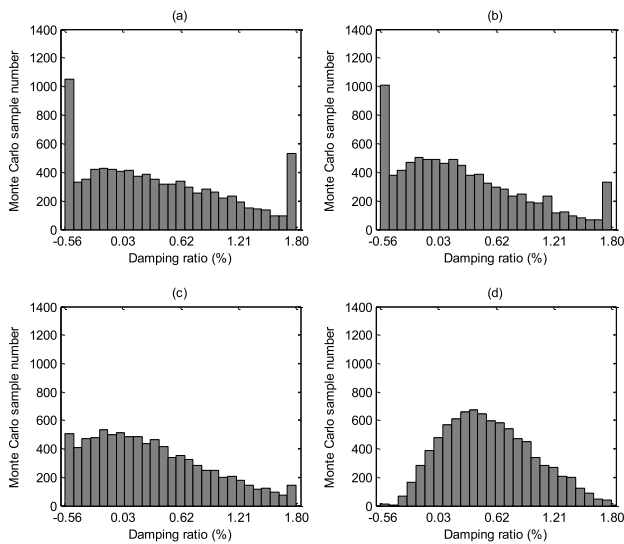


FIGURE 9. PDF of damping ratio of system critical oscillation mode for different scenarios of offshore wind power supply (B): (a) WF1 only; (b) WF2 only; (c) WF1+WF2; (d) WF1+WF2+WF3.

TABLE 5. Probabilistic stability of the test power system.

Wind power supply scenario	WF 1	WF2	WF1+W F2	WF1+WF2+W F3
Probability of damping ratio $\geq 0$	63.58 %	59.92 %	64.35%	88.83%

V. CONCLUSION

It has been known that the spatiotemporal complementarities of geographically dispersed wind can have the smoothing

effect on wind power output. This paper investigates the complementary effect of geographically distributed wind generation on power system economic and stable operation. The investigation was carried out in a real power system in China in terms of the unit commitment (UC) as well as the probabilistic small-signal angular stability. Real wind data provided by the China Meteorological Administration (CMA) were used in the UC and assessment of system probabilistic stability. Three offshore wind farms at different sites are combined to send wind power to the southern area in Jiangsu Province, China, via a multi-terminal DC (MTDC) network. Computational results of the UC and system probabilistic stability demonstrate that significant saving of operational cost of Jiangsu power system and reduction of probability of system instability can be brought about by the spatiotemporal complementarities of geographically distributed offshore wind farms. To the best knowledge of authors, it is the first time that the work presented in the paper has provided evidence of benefits of making use of spatiotemporal complementarities of wind generation to power system operation and stability.

APPENDIX A THE PARAMETERS OF SMALL SIGNAL STABILITY ANALYSIS

A small signal stability analysis model of AC test system in [41] is used in this paper. The parameters of the excitation system model of synchronous generators are

$$K_A = 7.4, T_A = 0.1s, V_{max} = 10.0, V_{min} = -10.0.$$

VSC-HVDC network data in p.u. are

$$R_{15} = 0.0006, R_{25} = 0.0006, R_{35} = 0.0006, R_{45} = 0.0006, R_{56} = 0.0012, R_{67} = 0.0006, R_{68} = 0.0006, R_{69} = 0.0006.$$

The VSC-converter model in [42] is applied for the converters and the loss of the converters is neglected. The parameters in p.u. are

$$R_c = 0.0001, X_c = 0.1643.$$

The DFIG model in [43] is used for wind farms and the parameters in p.u. are

$$D = 0.0, H = 1.7s, X_s = 0.29, X_r = 0.29, X_m = 2.6, R_s = 0.0, R_r = 0.0013.$$

The DFIG rotor-side converter controller in [16] is employed, in which  $K_P = 30, K_Q = 30$ .

APPENDIX B THE PARAMETERS OF WIND TURBINE

The parameters for the wind turbine used in this paper are:

- Nominal power: 3000 kW, Rotor diameter: 90 m,
- Nominal wind speed: 13 m/s, Maximum wind speed: 25 m/s,
- Hub height: 90 m, cut in wind speed: 3.5 m/s,

**APPENDIX C  
DERIVATION OF V-I DROOP TO DIVIDE WIND POWER**

In this paper, V-I droop Character of four converters are given in Fig. 10 and the steady-state DC equivalent circuit is shown in Fig. 11.

Assuming the proportion of wind power accommodated at four GSVSCs is  $n_1 : n_2 : n_3 : n_4$ , then

$$V_{dc2} - V_{dc1} = R_1 I_{dc1} - R_2 I_{dc2} \tag{34}$$

$$V_{dc2} - V_{dc1} = \frac{I_{dc2}}{k_2} - \frac{I_{dc1}}{k_1} \tag{35}$$

$$\frac{n_1}{n_2} = \frac{P_1}{P_2} \approx \frac{I_{dc1}}{I_{dc2}} \tag{36}$$

Through above three equations

$$k_2 = \frac{1}{\frac{n_1}{n_2}(R_1 + 1/k_1) - R_2} \tag{37}$$

Likewise,

$$k_3 = \frac{1}{\frac{n_1}{n_3}(R_1 + 1/k_1) - R_3} \tag{38}$$

$$k_4 = \frac{1}{\frac{n_1}{n_4}(R_1 + 1/k_1) - R_4} \tag{39}$$

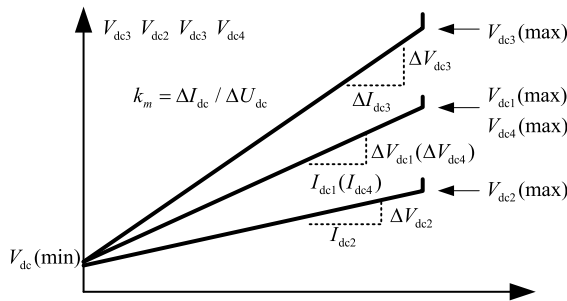


**FIGURE 10.** V-I characteristics for GSVSCs.

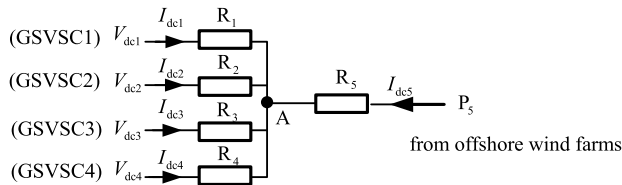


**FIGURE 11.** Steady-state DC equivalent circuit of the four-receiving-terminals.

**REFERENCES**

[1] A. Beluco, P. K. de Souza, and A. Krenzinger, "A dimensionless index evaluating the time complementarity between solar and hydraulic energies," *Renew. Energy*, vol. 33, no. 10, pp. 2157–2165, Oct. 2008.  
 [2] E. Kahn, "The reliability of distributed wind generators," *Electr. Power Syst. Res.*, vol. 2, no. 1, pp. 1–14, Mar. 1979.  
 [3] T. K. Simonsen and B. G. Stevens, "Regional wind energy analysis for the central United States," *Proc. Global Wind Power*, p. 16, 2004.  
 [4] J. Oswald, M. Raine, and H. Ashraf-Ball, "Will British weather provide reliable electricity?" *Energy Policy*, vol. 36, no. 8, pp. 3212–3225, Aug. 2008.

[5] G. Czisch and B. Ernst, "High wind power penetration by the systematic use of smoothing effects within huge catchment areas shown in a European example," *Windpower*, vol. 2001, 2001.  
 [6] D. A. Bechrakis and P. D. Sparis, "Correlation of wind speed between neighboring measuring stations," *IEEE Trans. Energy Convers.*, vol. 19, no. 2, pp. 400–406, Jun. 2004.  
 [7] G. Sinden, "Characteristics of the U.K. Wind resource: Long-term patterns and relationship to electricity demand," *Energy Policy*, vol. 35, no. 1, pp. 112–127, Jan. 2007.  
 [8] C. L. Archer and M. Z. Jacobson, "Supplying baseload power and reducing transmission requirements by interconnecting wind farms," *J. Appl. Meteorol. Climatol.*, vol. 46, no. 11, pp. 1701–1717, Nov. 2007.  
 [9] W. Kempton, F. M. Pimenta, D. E. Veron, and B. A. Colle, "Electric power from offshore wind via synoptic-scale interconnection," *Proc. Nat. Acad. Sci. USA*, vol. 107, no. 16, pp. 7240–7245, Apr. 2010.  
 [10] Y. Liu, L. Xiao, H. Wang, L. Lin, and S. Dai, "Investigation on the spatiotemporal complementarity of wind energy resources in China," *Sci. China Technol. Sci.*, vol. 55, no. 3, pp. 725–734, Mar. 2012.  
 [11] Y. Liu, L. Xiao, H. Wang, S. Dai, and Z. Qi, "Analysis on the hourly spatiotemporal complementarities between China's solar and wind energy resources spreading in a wide area," *Sci. China Technol. Sci.*, vol. 56, no. 3, pp. 683–692, Mar. 2013.  
 [12] H. Holttinen, V. B. Lemström, F. P. Meibom, and H. Bindner. (2007). *Design and Operation of Power Systems With Large Amounts of Wind Power*. State-of-the-Art Report. VTT (Espoo)(= VTT Work. Papers, 82). [Online]. Available: <http://www.ieawind.org/AnnexXXV/Publications> W  
 [13] A. Khodaei and M. Shahidehpour, "Transmission switching in security-constrained unit commitment," *IEEE Trans. Power Syst.*, vol. 25, no. 4, pp. 1937–1945, Nov. 2010.  
 [14] J. Wang, M. Shahidehpour, and Z. Li, "Security-constrained unit commitment with volatile wind power generation," *IEEE Trans. Power Syst.*, vol. 23, no. 3, pp. 1319–1327, Aug. 2008.  
 [15] F. D. Galiana, A. J. Conejo, and H. A. Gil, "Transmission network cost allocation based on equivalent bilateral exchanges," *IEEE Trans. Power Syst.*, vol. 18, no. 4, pp. 1425–1431, Nov. 2003.  
 [16] S. Bu, W. Du, H. Wang, Z. Chen, L. Xiao, and H. Li, "Probabilistic analysis of small-signal stability of large-scale power systems as affected by penetration of wind generation," *IEEE Trans. Power Syst.*, vol. 27, no. 2, pp. 762–770, May 2012.  
 [17] E. Hinrichsen and P. Nolan, "Dynamics and stability of wind turbine generators," *IEEE Trans. Power App. Syst.*, vol. PAS-101, no. 8, pp. 2640–2648, Aug. 1982.  
 [18] F. Mei and B. C. Pal, "Modelling of doubly-fed induction generator for power system stability study," in *Proc. Power Energy Soc. Gen. Meeting Convers. Del. Electr. Energy 21st Century*, Jul. 2008, pp. 1–8.  
 [19] L. Xu and B. R. Andersen, "Grid connection of large offshore wind farms using HVDC," *Wind Energy*, vol. 9, no. 4, pp. 371–382, 2006.  
 [20] J. Li, P. Shi, and H. Gao, "China wind power outlook," Chin. Renew. Energy Industries Assoc. Global Wind Energy Council Greenpeace, Tech. Rep., 2010.  
 [21] N. P. Padhy, "Unit commitment-a bibliographical survey," *IEEE Trans. Power Syst.*, vol. 19, no. 2, pp. 1196–1205, May 2004.  
 [22] U. A. Ozturk, M. Mazumdar, and B. A. Norman, "A solution to the stochastic unit commitment problem using chance constrained programming," *IEEE Trans. Power Syst.*, vol. 19, no. 3, pp. 1589–1598, Aug. 2004.  
 [23] Y. V. Makarov, C. Loutan, J. Ma, and P. D. Mello, "Operational impacts of wind generation on California power systems," *IEEE Trans. Power Syst.*, vol. 24, no. 2, pp. 1039–1050, May 2009.  
 [24] A. Fabbri, T. G. S. Roman, J. R. Abbad, and V. H. M. Quezada, "Assessment of the cost associated with wind generation prediction errors in a liberalized electricity market," *IEEE Trans. Power Syst.*, vol. 20, no. 3, pp. 1440–1446, Aug. 2005.  
 [25] U. Focken and M. Lange, *Physical Approach to Short-Term Wind Power Prediction*. Springer, 2006.  
 [26] U. Focken, M. Lange, K. Mönnich, H.-P. Waldl, H. G. Beyer, and A. Luig, "Short-term prediction of the aggregated power output of wind farms—A statistical analysis of the reduction of the prediction error by spatial smoothing effects," *J. Wind Eng. Ind. Aerodynamics*, vol. 90, no. 3, pp. 231–246, Mar. 2002.  
 [27] F. Bouffard and F. D. Galiana, "Stochastic security for operations planning with significant wind power generation," in *Proc. IEEE Power Energy Soc. Gen. Meeting Convers. Del. Electr. Energy 21st Century*, Jul. 2008, pp. 1–11.

- [28] G. Strbac, A. Shakoor, M. Black, D. Pudjianto, and T. Bopp, "Impact of wind generation on the operation and development of the U.K. Electricity systems," *Electr. Power Syst. Res.*, vol. 77, no. 9, pp. 1214–1227, 2007.
- [29] M. Carrión and J. M. Arroyo, "A computationally efficient mixed-integer linear formulation for the thermal unit commitment problem," *IEEE Trans. Power Syst.*, vol. 21, no. 3, pp. 1371–1378, Jul. 2006.
- [30] M. H. Albadi and E. F. El-Saadany, "Comparative study on impacts of wind profiles on thermal units scheduling costs," *IET Renew. Power Gener.*, vol. 5, no. 1, pp. 26–35, Nov. 2011.
- [31] A. Lotfjou, M. Shahidehpour, Y. Fu, and Z. Li, "Security-constrained unit commitment with AC/DC transmission systems," *IEEE Trans. Power Syst.*, vol. 25, no. 1, pp. 531–542, Feb. 2010.
- [32] B. A. McCarl, A. Meeraus, P. van der Eijk, M. Bussieck, S. Dirkse, P. Steacy, and F. Nelissen, "McCarl GAMS user guide," GAMS Develop. Corp., Tech. Rep., 2013.
- [33] P. Meibom, R. Barth, H. Brand, and C. Weber, "Wind power integration studies using a multi-stage stochastic electricity system model," in *Proc. Power Eng. Soc. Gen. Meeting*, Jun. 2007, pp. 1–4.
- [34] I. Tekdemir and V. Genc, "A small-signal stability related probabilistic security assessment of wind power integration into power systems," in *Proc. 7th Int. Conf. Elect. Electron. Eng. (ELECO)*, Dec. 2011, pp. 1-211–I-214.
- [35] C. Wang, L. Shi, L. Yao, L. Wang, Y. Ni, and M. Bazargan, "Modelling analysis in power system small signal stability considering uncertainty of wind generation," in *Proc. IEEE PES Gen. Meeting*, Jul. 2010, pp. 1–7.
- [36] R. W. Garvine and W. Kempton, "Assessing the wind field over the continental shelf as a resource for electric power," *J. Mar. Res.*, vol. 66, no. 6, pp. 751–773, Nov. 2008.
- [37] R. J. Barthelmie, M. S. Courtney, J. Højstrup, and S. E. Larsen, "Meteorological aspects of offshore wind energy: Observations from the vindeby wind farm," *J. Wind Eng. Ind. Aerodyn.*, vol. 62, nos. 2–3, pp. 191–211, Sep. 1996.
- [38] W. Kempton, C. L. Archer, A. Dhanju, R. W. Garvine, and M. Z. Jacobson, "Large CO<sub>2</sub> reductions via offshore wind power matched to inherent storage in energy end-uses," *Geophys. Res. Lett.*, vol. 34, no. 2, pp. 1–5, 2007.
- [39] N. G. Mortensen, D. Heathfield, L. Landberg, O. Rathmann, I. Troen, and E. Petersen, "Wind atlas analysis and application program: WAsP 7. Version 7.1: Help facility," Tech. Rep., 2000.
- [40] R. J. Barthelmie, G. C. Larsen, S. T. Frandsen, L. Folkerts, K. Rados, S. C. Pryor, B. Lange, and G. Schepers, "Comparison of wake model simulations with offshore wind turbine wake profiles measured by sodar," *J. Atmos. Ocean. Technol.*, vol. 23, no. 7, pp. 888–901, Jul. 2006.
- [41] W. Du, H. Wang, and L. Y. Xiao, "Power system small-signal stability as affected by grid-connected photovoltaic generation," *Eur. Trans. Electr. Power*, vol. 22, pp. 688–703, Jul. 2012.
- [42] J. Beerten, S. Cole, and R. Belmans, "Generalized steady-state VSC MTDC model for sequential AC/DC power flow algorithms," *IEEE Trans. Power Syst.*, vol. 27, no. 2, pp. 821–829, May 2012.
- [43] H. Akagi and H. Sato, "Control and performance of a doubly-fed induction machine intended for a flywheel energy storage system," *IEEE Trans. Power Electron.*, vol. 17, no. 1, pp. 109–116, Jan. 2002.

**JING ZHOU** is currently working at Three Gorges Power Company Ltd. Her research interests include the economic analysis and the operation of PV generation.

**YI LIU** received the B.S. degree from the School of Electrical Engineering, Tianjin University, China, and the Ph.D. degree from the Institution of Electrical Engineering, Chinese Academic of Science.

His research interests include the economic and stability analysis of power system operation, including renewable power, and multi-terminal DC power systems.

**ZHE KANG** is currently working at Three Gorges Power Company Ltd. His research interests include the economic analysis and the operation of PV generation and operation of the micro-grid.

**ZHUOYU JIANG** is currently working at Three Gorges Power Company Ltd. His research interests include the economic analysis and the operation of the micro-grid.

• • •